Doubly-resonant sum-frequency generation spectroscopy for surface studies

M. B. Raschke, and Y. R. Shen

Department of Physics, University of California,

and Materials Sciences Division, Lawrence Berkeley National Laboratory,

Berkeley, California 94720

M. Hayashi

Center for Condensed Matter Sciences, National Taiwan University, Taipei, Taiwan

S. H. Lin

Institute of Atomic and Molecular Sciences, Academia Sinica, Taipei, Taiwan

Abstract

Doubly-resonant infrared-visible sum-frequency generation (DR-SFG) as a two-dimensional surface spectroscopy was demonstrated experimentally for the first time. Probing electronic and vibrational transitions of a surface molecular monolayer simultaneously, the technique gives access to information about the electron-vibration coupling of the surface molecules. It allows more selective studies of any interface accessible by light.

Second-harmonic and sum-frequency generation (SHG/SFG) have found a wide range of applications as probes in surface science due to their intrinsic surface and interface sensitivity and specificity [1–5]. In particular, infrared-visible SFG has emerged as a versatile spectroscopic technique applicable to such diverse systems as polymer, semiconductor and metal surfaces, heterogeneous catalysis, electrochemistry and liquid interfaces. In that process, two input beams, one visible at $\omega_{\rm vis}$ and the other infrared at $\omega_{\rm IR}$, overlap on the surface of the material being investigated and the sum-frequency generation, typically in reflection, at $\omega_{\rm s} = \omega_{\rm vis} + \omega_{\rm IR}$ is detected. When $\omega_{\rm IR}$ is tuned over vibrational resonances the SF output exhibits resonant enhancement. The obtained vibrational spectrum provides information about surface composition and structure, as well as surface dynamical properties via time-dependent measurements.

With both $\omega_{\rm IR}$ and $\omega_{\rm vis}$ near surface vibrational and electronic transitions, respectively, SFG could be doubly resonantly enhanced [6]. In this respect it is similar to Resonance Raman Spectroscopy (RRS), known for its applications in condensed matter physics, chemistry, and biology, but SFG has the additional virtue of being surface-specific. Analogous to RRS, doubly resonant (DR) enhancement in SFG only occurs when the corresponding vibrational and electronic transitions are coupled. This allows for more selective spectroscopic information and better assignment of the surface modes. It permits deduction of the coupling strengths between various electronic and vibrational transitions. The new technique could also be valuable for studies of inter-molecular interactions at surfaces and interfaces.

Here we report on the first experiment on DR-SFG. While the technique is generally applicable to any interface accessible by light, including those between two pure media, we used adsorbed monolayers of Rhodamine 6G (Rh6G) as an example to demonstrate the principles of this technique. Doubly-resonant enhancement from coupled electronic and vibrational transitions of Rh6G was observed. It exhibited an unprecedented surface sensitivity. From the DR-SFG spectra relative electron-vibration coupling strengths between different vibrational modes and the S_0-S_1 electronic resonance of Rh6G were deduced.

Let us first describe briefly the theory of DR-SFG. In the electric-dipole approxima-

tion, surface SFG from a material with inversion symmetry arises from the second-order polarization

$$\mathbf{P}^{(2)}(\omega_{\rm s}=\omega_{\rm vis}+\omega_{\rm IR})=\epsilon_0\boldsymbol{\chi}^{(2)}(\omega_s):\mathbf{E}(\omega_{\rm vis})\mathbf{E}(\omega_{\rm IR}), \tag{1}$$

induced by the input fields $\mathbf{E}(\omega_{\rm vis})$ and $\mathbf{E}(\omega_{\rm IR})$ at the surface, where $\boldsymbol{\chi}^{(2)}$ denotes the second-order surface nonlinear susceptibility tensor [7,8]. In the infrared-visible DR-SFG case, the microscopic expression for $\boldsymbol{\chi}^{(2)}$ is dominated by a single doubly-resonant term [6,9,10]. Considering the IR-vis DR-SFG process shown schematically in Fig. 1 one finds,

$$\chi^{(2)}_{ijk}=-\frac{N}{\hbar^2}\left\langle\sum_{b,n}\frac{\langle\psi_{g0}|\mu_i|\psi_{en}\rangle\langle\psi_{en}|\mu_j|\psi_{gb}\rangle\langle\psi_{gb}|\mu_k|\psi_{g0}\rangle}{(\omega_{\rm s}-\omega_{en,g0}+i\Gamma_{en,g0})(\omega_{\rm IR}-\omega_{gb,g0}+i\Gamma_{gb,g0})}\right\rangle+\left(\chi^{(2)}_{\rm NR}\right)_{ijk}, \tag{2}$$

where N is the surface molecular density, μ the electric-dipole operator, b, n, and g, e label vibrational and electronic states, respectively, with $\omega_{en,g0}$, $\omega_{gb,g0}$, and $\Gamma_{en,g0}$, $\Gamma_{gb,g0}$ denoting transition frequencies and damping constants, respectively, the angular brackets represent an average over molecular orientations, and $(\chi^{(2)}_{\rm NR})_{ijk}$ describes the off-resonant contributions. Under the Born-Oppenheimer approximation $\langle\psi_{gb}|\mu_k|\psi_{g0}\rangle\simeq(\partial\mu^k_{gg}/\partial q)\langle gb|q|g0\rangle$ Eq. 2 becomes

$$\chi^{(2)}_{ijk}=-\frac{N}{\hbar^2}\left\langle\sum_{b,n}\mu^i_{eg}\mu^j_{ge}\frac{\partial\mu^k_{gg}}{\partial q}\frac{\langle g0|ev\rangle\langle ev|gb\rangle\langle gb|q|g0\rangle}{(\omega_s-\omega_{en,g0}+i\Gamma_{en,g0})(\omega_{\rm IR}-\omega_{gb,g0}+i\Gamma_{gb,g0})}\right\rangle+\left(\chi^{(2)}_{\rm NR}\right)_{ijk}. \tag{3}$$

For explicit evaluation of Eq. 3, we use a simple model to describe the states involved in the DR process [6]. Each vibrational mode is treated as a harmonic oscillator linearly coupled with the electronic ground and excited states, $|g\rangle$ and $|e\rangle$. The electron-vibration coupling then results in a displacement d between the two vibrational potential energy curves $E_g(q)$ and $E_e(q)$ along the vibrational coordinate q (see Fig. 1). $d=a\sqrt{\hbar/\omega_Q}$ with a being the dimensionless Franck-Condon electron-vibration coupling coefficient and ω_Q the frequency of the Q-th vibrational mode. For simplicity we assume here that the vibrational mode frequencies remain the same for the electronic ground and excited states, but this assumption, as well as the assumption of linear electron-phonon coupling, can be relaxed readily [9,11]. The vibrational wavefunctions associated with the electronic ground and excited states are

then given by the eigenfunctions of a harmonic oscillator in the appropriate normal coordinates, $\phi_i(q)$ and $\phi_j(q+d)$ for $|gi\rangle$ and $|ej\rangle$, respectively. Consequently, the matrix elements in the summation of Eq. 3 can be explicitly calculated. We obtain [12]

$$\chi^{(2)}_{ijk} = -\frac{N}{\hbar^2}\left\langle \sum_Q \mu^i_{eg}\mu^j_{ge}\frac{\partial \mu^k_{gg}}{\partial q}\frac{\sqrt{S}e^{-S}}{\omega_{\rm IR}-\omega_Q+i\Gamma_Q} \right.$$
$$\left. \times \sum_{n=0}^{\infty}\frac{S^n}{n!}\left\{\frac{1}{\omega_s - n\omega_Q - \omega_{eg} + i\Gamma_{en,g0}} - \frac{1}{\omega_s-(n+1)\omega_Q-\omega_{eg}+i\Gamma_{en+1,g0}}\right\}\right\rangle + (\chi^{(2)}_{\rm NR})_{ijk}, \quad (4)$$

where $S = d^2\omega_Q/2\hbar$, known as the Huang-Rhys factor, is related to a by $S = a^2/2$. We shall use Eq. 4 to fit the experimental DR-SFG spectra and deduce the coupling strengths S in the data analysis.

In our experiment, we used a homogeneous monolayer of Rhodamine 6G dye molecules on a fused silica substrate as a representative system. Rh6G was chosen because its spectral characteristics are well understood from extensive spectroscopic studies in the past [13–16]. The samples were prepared by spin-coating a 0.3 mM ethanolic solution resulting in a surface molecular density of 3×10^{13} cm^{-2}, as determined by visible absorption measurements.

For the DR-SFG experiments, tunable IR and visible light was provided by two optical parametric generator/amplifier systems pumped by a Nd:YAG laser with an 18 ps pulsewidth and a 20 Hz repetition rate [17]. The two input pulses were overlapped on the sample with incident angles of $\beta_{\rm IR} = 40°$ and $\beta_{\rm vis} = 50°$. The SFG output was detected in the reflected direction after spatial and spectral filtering. The combined maximum input fluence on the sample was limited to 100 mJ/cm^2 off the Rh6G S_0-S_1 absorption band and to 20 mJ/cm^2 near it to avoid laser heating or photo-induced reactions. The SFG spectra were reproducible within 20% from measurements on different samples. The SFG output was normalized against that from a z-cut quartz crystal allowing for the determination of absolute values of $|\chi^{(2)}_{ijk}|$.

DR-SFG spectroscopy was performed by tuning $\omega_{\rm IR}$ over vibrational resonances of Rh6G in the 1500-1750 cm^{-1} range and keeping $\omega_{\rm vis}$ fixed at different values. The visible frequencies $\omega_{\rm vis}$ were chosen such that they cover the S_0-S_1 absorption peak. A representative set of spectra obtained with the *ssp* (s-, s-, and p-polarizations for SF, visible, and IR fields,

respectively) polarization combination is shown in Fig. 2. In each spectrum four distinct peaks appear. Those at 1514, 1573, and 1657 cm^{-1} can be attributed to the xanthene skeleton vibrational modes of Rh6G and the one at 1614 cm^{-1} to the phenyl group attached to the xanthene [15]. All of them exhibit a pronounced variation in their peak intensities as ω_{vis} is varied. The maximum value of $\chi^{(2)}$ at the peak of the 1657 cm^{-1} resonance is $\sim 4.7 \times 10^{-20}$ m^2/V as compared to $\sim 7 \times 10^{-22}$ m^2/V for a stretch mode of a typical CH-group of equivalent surface density measured by conventional singly-resonant SFG.

To analyze the spectra, we note that with the visible input frequency ω_{vis} fixed, Eq. 3 or 4 can be approximated by the form

$$\chi^{(2)}_{ijk} = \sum_{Q} \frac{A_Q}{\omega_{IR} - \omega_Q + i\Gamma_Q} + \chi^{(2)}_{NR}, \tag{5}$$

We use Eq. 5 to fit all the measured spectra with ω_Q, Γ_Q, A_Q and $\chi^{(2)}_{NR}$ as adjustable parameters. For each vibrational mode, ω_Q and Γ_Q are taken as independent of ω_s, but A_Q and $\chi^{(2)}_{NR}$ do vary with ω_s. The results are displayed in Fig. 3 where A_Q is plotted versus ω_s for three vibrational modes. We refer to these curves as the excitation spectra for the DR-SFG process involving the vibrational modes. As expected, all the excitation spectra exhibit a resonance coincident with the S_0-S_1 linear absorption peak for the Rh6G monolayer, which is plotted for comparison.

It can be seen that the absorption peak in Fig. 3 shows a longer tail on the high-frequency side than the peak in the excitation spectra. This is due to contributions from vibronic transitions involving coupled vibrational modes in the absorption. One would expect these transitions to also contribute to the excitation spectra of DR-SFG: In Eq. 4 there are successive resonant terms describing ω_s in resonance with vibronic transitions with frequencies $\omega_{eg} + n\omega_Q$ for $n = 0, 1, 2$, etc. Although their amplitude drops off rapidly with increasing $n > 1$, for small electron-phonon coupling one would expect to see the $n = 1$ vibrational sideband in the excitation spectrum (see also below). However, this was not clearly observed in our experiment. Presumably the reason is that the vibronic transitions of Rh6G have significantly shorter dephasing times [14], so that the corresponding larger damping constants

($\Gamma_{\mathrm{en,g0}}$ in Eq. 4) or spectral widths would suppress the resonant contributions, with respect to $\chi^{(2)}_{\mathrm{NR}}$ in Eq. 5, below the discernible level.

We can deduce an explicit expression for $A_Q(\omega_s)$ by comparing Eq. 4 with Eq. 5. To fit the observed excitation spectra, we use, for each vibrational mode Q, S and $\Gamma_{\mathrm{en,g0}}$ as adjustable parameters. The zero-vibration S_0-S_1 transition frequency, ω_{eg}, is taken as 18,400 cm^{-1} (2.28 eV). We find that a good description of the observed excitation spectrum for the 1657 cm^{-1} mode requires $\Gamma_{\mathrm{e0,g0}} = (500 \pm 50)$ cm^{-1} and $\Gamma_{\mathrm{en,g0}} = (2 \pm 0.4)\Gamma_{\mathrm{e0,g0}}$ for $n \geq 1$ (Fig. 3a, solid line). For comparison, using $\Gamma_{\mathrm{e1,g0}} = \Gamma_{\mathrm{e0,g0}}$, we obtain the dashed curve for $A_Q(\omega_s)$. The other three vibrational modes, require $\Gamma_{\mathrm{e0,g0}} = (500 \pm 50)$ cm^{-1} and $\Gamma_{\mathrm{en,g0}} \gtrsim 3\Gamma_{\mathrm{e0,g0}}$ for $n \geq 1$ to fit the experimental data (Fig. 3b). These results indicate that the vibronic transitions have shorter dephasing times than the zero-vibration transition. Early measurements found that the dephasing times of vibronic transitions of Rh6G are less than 30 fs [14]. The larger $\Gamma_{\mathrm{en,g0}}$ will also suppress the resonant enhancement of DR-SFG that starts with an electronic transition followed by a vibrational transition in the electronic excited state (see Fig. 1). Indeed this process was not observed, and has been neglected in the derivation of Eq. 3-4.

Without being able to resolve the vibronic sidebands in our excitation spectra, except for setting an upper limit of $S \sim 0.2$ for the 1657 cm^{-1} mode, we cannot determine the absolute values of S for the vibrational modes of Rh6G. We can, however, obtain relative values of S, using relative values of $\partial\mu_{gg}/\partial q$ in Eq. 4 for the different modes. The latter were deduced from an infrared absorption measurement of Rh6G dissolved in solid KBr and are summarized in Table I together with the resulting values for S_{rel}. Fig. 4 then presents the calculated two-dimensional DR-SFG spectrum using these tabulated parameters.

For Rh6G, the S_0-S_1 electronic transition is dominated by the $\pi - \pi^*$ excitation of the large xanthene group of the molecule. As mentioned earlier the vibrational mode at 1614 cm^{-1} can be assigned to the pendant phenyl group while those at 1514, 1573 and 1657 cm^{-1} directly to the xanthene group. They are expected to have different degrees of coupling with the electronic transition. In agreement with the results from Resonance Raman experiments from Rh6G in solution [15,16] the 1614 cm^{-1} mode has the smallest coupling strength because

the phenyl ring is external to the xanthene group and is rotated out of the molecular plane. Despite the small coupling strength, the mode still has the strongest peak intensity in the SFG spectra since it has the largest IR absorption strength of all vibrational modes of Rh6G.

In summary, we have performed the first DR-SFG experiment and shown that it is a viable two-dimensional surface spectroscopic technique. In much the same way as multi-dimensional spectroscopy is suitable for studies of intra- and inter-molecular interactions in the bulk, DR-SFG provides a similar opportunity for studies of molecules at surfaces. In our experiment, the doubly resonant enhancement allowed deduction of couplings between electronic transitions and vibrational modes. Although the experiment reported here is on adsorbed molecular monolayer, the technique can be extended to studies of interaction between any pairs of surface resonances and is applicable to all surfaces and interfaces accessible by light, including those of neat liquids and solids.

The authors acknowledge valuable discussions with J. McGuire and X. Wei. This work was supported by the Director, Office of Energy Research, Office of Basic Energy Sciences, Materials Science Division of the U.S. Department of Energy under Contract No. DE-AC03-76SF00098, and a Max-Planck Society Research Award. SHL and MH thank the NSC of ROC and Academia Sinica, and MBR thanks the Alexander von Humboldt Foundation and the Max-Planck Society for financial support.

REFERENCES

[1] T. F. Heinz, in *Nonlinear surface electromagnetic phenomena*, ed. by H.-E. Ponath and G. I. Stegeman, North-Holland, Amsterdam, 1991, p. 353.

[2] Y. R. Shen, in *Frontiers in laser spectroscopy*, ed. T. W. Hänsch and M. Inguscio (North-Holland, Amsterdam, 1994), p.139.

[3] P. Guyot-Sionnest and A. L. Harris, in *Laser Spectroscopy and Photochemistry on Metal Surfaces*, ed. H.-L. Dai and W. Ho (World Scientific, Singapore, 1995). J. Y. Huang and Y. R. Shen, *ibid.*

[4] P. Dumas, M. K. Weldon, Y. J. Chabal, and G. P. Williams, Surf. Rev. Lett. **6**, 225 (1999).

[5] E. Matthias and F. Träger, editors, Appl. Phys. B, Special Issue: *Nonlinear optics at interfaces*, Vol. 210, No. 3 (1999).

[6] Jung Y. Huang and Y. R. Shen, Phys. Rev. A, **49**, 3973 (1994).

[7] N. Bloembergen, *Nonlinear Optics* (Benjamin, New York, 1977). Y. R. Shen, *The principles of nonlinear optics* (Wiley, New York, 1984).

[8] We use MKS units and follow the convention of separating ϵ_0 from χ.

[9] J. C. Vallet, A. J. Boeglin, J. P. Lavoine, and A. A. Villaeys, Phys. Rev. A, **53**, 4508 (1996).

[10] S. H. Lin, M. Hayashi, R. Islampour, J. Yu, D. Y. Yang, and George Y. C. Wu, Physics B, **222**, 191 (1996).

[11] R. Islampour, M. Hayashi, and S. H. Lin, Chem. Phys. Lett. **234**, 7 (1995).

[12] E. Hutchisson, Phys. Rev. **36**, 410 (1930). H. Kuzmany, *Solid-state spectroscopy* (Springer, Berlin, 1998).

[13] T. F. Heinz, C. K. Chen, D. Ricard, and Y. R. Shen, Phys. Rev. Lett. **48**, 478 (1982).

[14] C. V. Shank, E. P. Ippen, and O. Teschke, Chem. Phys. Lett. **45**, 291 (1977). A. J. Taylor, D. J. Erskine, and C. L. Tang, *ibid.*, **103**, 430 (1984).

[15] P. Hildebrandt and M. Stockburger, J. Phys. Chem. **88**, 5935 (1984). M. Majoube, and M. Henry, Spectrochimica Acta, **47**, 1459 (1991).

[16] M. Takayanagi, H. Hamaguchi, and M. Tasumi, Chem. Phys. Lett. **128**, 555 (1986).

[17] J. Y. Zhang, J. Y. Huang, Y. R. Shen, and C. Chen, J. Opt. Soc. Am. B, **10**, 1758 (1993).

TABLES

$\omega_{\mathrm{g1,g0}}$ (cm^{-1})	$\Gamma_{\mathrm{g1,g0}}$ (cm^{-1})	$\partial\mu_{gg}/\partial q$	S_{rel}
1514	8	4.5	0.02
1573	8	0.8	0.25
1614	8	7.5	0.005
1657	9	1.0	1.0
$\omega_{\mathrm{e0,g0}}$ (cm^{-1})	$\Gamma_{\mathrm{e0,g0}}$ (cm^{-1})	$\Gamma_{\mathrm{en(n\geq 1),g0}}$ (cm^{-1})	
18400	500	1000-1500	

TABLE I. Result of best fit to the DR-SFG experimental data from calculations described in the text. $\partial\mu_{gg}/\partial q$ denotes relative infrared vibrational intensities. The parameter S_{rel} refers to the relative electron-vibration coupling constant.

FIGURES

FIG. 1. Model adiabatic potentials for molecular electronic ground and excited states as functions of configurational coordinate q. The doubly-resonant IR-vis (and vis-IR) sum-frequency generation processes are shown schematically.

FIG. 2. Doubly-resonant sum-frequency spectra of a molecular monolayer of Rhodamine 6G molecules on fused quartz in *ssp* polarization combination normalized against the signal from a z-cut quartz. The solid lines were derived from a numerical fit using Eq. 5.

FIG. 3. Excitation spectra of DR-SFG for three vibrational modes of Rh6G plotted as a function of the sum-frequency photon energy (open symbols) in comparison with the linear absorption spectrum (dots). The solid and dashed lines are numerical fits using the model described in the text.

FIG. 4. Simulated DR-SFG spectrum of Rh6G using the parameters given in Table I.

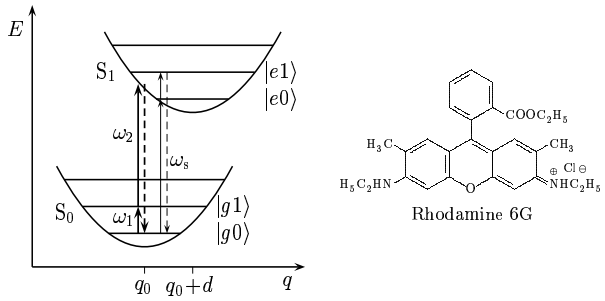
E
S1
|e1⟩
|e0⟩
ω2
ωs
S0
ω1
|g1⟩
|g0⟩
q0
q0+d
q
COOC2H5
H3C
CH3
H5C2HN
Cl⊖
NHC2H5
O
Rhodamine 6G

FIG. 1.

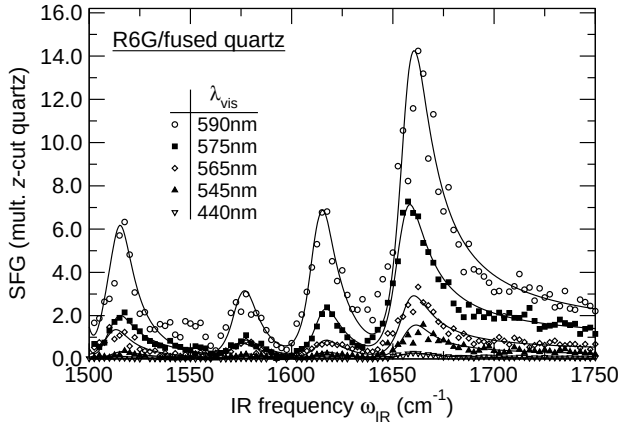
R6G/fused quartz
λvis
590nm
575nm
565nm
545nm
440nm
SFG (mult. z-cut quartz)
IR frequency ωIR (cm-1)
16.0
14.0
12.0
10.0
8.0
6.0
4.0
2.0
0.0
1500
1550
1600
1650
1700
1750

FIG. 2.

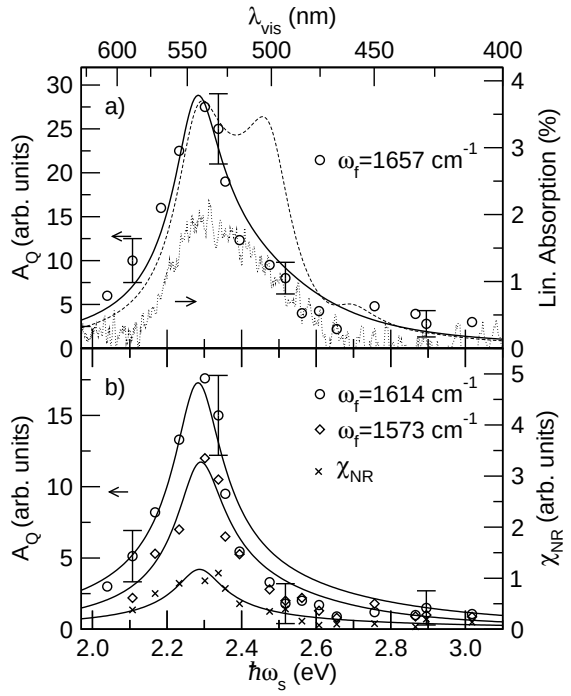
λvis (nm)
600
550
500
450
400
a)
ωf=1657 cm-1
AQ (arb. units)
Lin. Absorption (%)
b)
ωf=1614 cm-1
ωf=1573 cm-1
χNR
χNR (arb. units)
ħωs (eV)
2.0
2.2
2.4
2.6
2.8
3.0

FIG. 3.

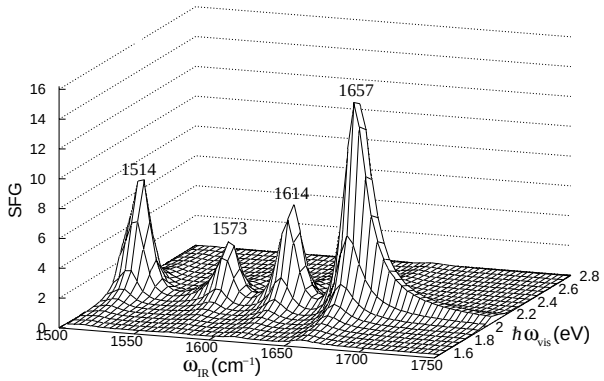
SFG
1657
1514
1614
1573
ωIR (cm-1)
1500
1550
1600
1650
1700
1750
ħωvis (eV)
1.6
1.8
2
2.2
2.4
2.6
2.8

FIG. 4.